Detailing, a key element in the robustness of concrete composite floors

Jules Smits
PhD researcher, KU Leuven, Dept. of Civil Engineering, Sint-Katelijne-Waver, Belgium

Ann Van Gysel
Professor, KU Leuven, Dept. of Civil Engineering, Sint-Katelijne-Waver, Belgium

Stijn François
Professor, KU Leuven, Dept. of Civil Engineering, Leuven, Belgium

Tom Molkens
Professor, KU Leuven, Dept. of Civil Engineering, Sint-Katelijne-Waver, Belgium

ABSTRACT: In 2017, a parking building under construction collapsed in Eindhoven, the Netherlands. The possible cause is failure of the composite flooring system. Rather coincidentally, just before the collapse, a research campaign was launched at KU Leuven to unravel the joint action in the type of composite flooring used. Such a concrete floor system, according to EN 13747, consists of a prefabricated lower shell and a thicker top layer poured on site, which also contains the overlap reinforcement between the different prefabricated plates. From the test campaign, it became clear that, during the development of any alternative load bearing paths, the composite action can be analyzed using the theory of strength of materials. The transfer of forces by reinforcement is only possible as long as the precast slab and the second phase concrete remain in contact, and for this, the function of the lattice girders is of prime importance. In this sense, it should be regarded that correct detailing rules should be developed for different structural systems to avoid localized failure, affecting a negative impact on the development of alternative load paths.

1. INTRODUCTION

To meet ductility requirements in the framework of robustness, it should be avoided that (brittle) joint behavior becomes decisive in the failure of a structural element. For composite floors made with precast floor plates, avoiding brittle joint failure further allows to limit the consequences of thermal effects, differential settlements, shrinkage, and creep (CEN 2005).

The requirements to achieve robustness are included in NBN EN 1990 (CEN 2002) section 2.1 and are reproduced as follows: a structure shall be designed and executed in such a way that it will not be damaged by accidental actions (explosions, impact, and the consequences of human errors) to an extent disproportionate to the original cause.

Unfortunately, neglecting this sound engineering principle may have resulted in a partial collapse of a parking building of Eindhoven Airport in the Netherlands (Linssen 2019).

The robustness of a system can be experimentally tested by performing a *column loss scenario* (O'Connor et al. 2021). Some of these tests have been performed on full-scale reinforced concrete frame structures by (Sasani et al. 2007), (Sasani 2008), (Sasani and Sagiroglu 2010), (Keyvani and Sasani 2015) and (Adam et al. 2020), providing insight into the mechanisms that act in the case of a progressive collapse. In addition to tests on frame structures, experiments are also conducted on elements, for example by (Botte et al. 2015). For precast elements, some

tests have already been completed on hollow cores by (Michelini et al. 2020).

Due to the removal of a column, a load redistribution occurs. This includes the change of bending moments, which can cause higher tension forces in the floor plate reinforcement as long as the bending theory is valid (approximately till the vertical deflection is limited to half of the floor thickness). If not, and if the boundary conditions allow it, catenary action occurs and the entire section is subjected to tensile forces. Such action is particularly challenging for a floor system made of prefabricated floor plates, as this implies the presence of joints where overlap bars need to transfer forces between these floor plates. It can be noted that this type of overlap is not covered by the code regulations as they presume always overlaps in the same layer of reinforcement and certainly not an overlap where the equilibrium of forces must be guaranteed crossing an interface between two stages of concrete. Due to a difference in stiffness at the location of the joint, a possible delamination effect is occurring (Molkens and Van Gysel 2022), which makes that the joint reinforcement must be sufficiently large, and most important which puts forward the contribution of the lattice girders.

In the heavily delaminated zone in the close neighborhood of the joint, shear stresses cannot be transferred between the joint and floor plate reinforcement, so the overlap length is not valid here. None of the three involved mechanisms (adhesion, friction, and mechanical interlock) at an interface are still available. At the location of the first lattice girder near the joint, the delamination is stopped or strongly reduced, and therefore the overlap length starts only at the center of this lattice girder (Molkens and Van Gysel 2021).

So, a lattice girder is a key element in the behavior of the joint and has a major importance on the detailing of concrete composite floors. The design of this lattice girder requires knowledge about the action effects on this element, which is the scope of this research. Various measurement methods on real-scale elements are proposed and discussed, as is the influence of the bonding surface between both concrete phases.

2. CODE REVIEW

2.1. NBN EN 1991-1-7

NBN EN 1991-1-7 (CEN 2006) dealing with accidental loads almost exactly repeats the already mentioned phrase out of NBN EN 1990 (CEN 2002). It can be highlighted that this is the only place in all Eurocodes where the effects of human error (in design and/or execution) are covered.

To obtain robustness, some methods and strategies are described in this document. A distinction is made between identified (e.g. explosions or impact) and unidentified accidental actions. A classical structural analysis may be used in case of identified accidental actions. Annex A of NBN EN 1991-1-7 (CEN 2006) describes the measures for unidentified actions, which depend on the consequences of an accident (classification of buildings in consequences classes) (Gulvanessian and Vrouwenvelder 2006). For buildings in consequence class 2b, column loss tests should determine whether a certain limit of local damage is exceeded. If not, the building will survive a reasonable range of unidentified actions, and adequate robustness is obtained.

A strategy to provide acceptable robustness of a structure is the application of tying systems (Art. 2.3). However the joint detail should allow also for the development of alternative load paths when needed.

2.2. NBN EN 1992-1-1

Robustness requirements of concrete structures are addressed in Art. 9.10 of NBN EN 1992-1-1 (CEN 2005). It is cited that a structure shall have a suitable tying system to withstand accidental actions and prevent a progressive collapse. These tying systems will provide an alternative load path after local damage occurs (CEN 2005).

2.3. Horizontal tying in NBN EN 1991-1-7 and NBN EN 1992-1-1

NBN EN 1991-1-7 (CEN 2006) and NBN EN 1992-1-1 (CEN 2005) mention that a peripheral tie should be capable of respectively resisting a tensile force T_p (Eq. (1)) or $F_{tie,\,per}$ (Eq. (2)).

$$T_p = max\{0.4(g_k + \psi g_k)sL; 75\ kN\} \quad (1)$$

$$F_{tie,per} = l_i \cdot q_1 \leq q_2 \quad (2)$$

NBN EN 1992-1-1 (CEN 2005) recommends a value of 70 kN for q_2 in Eq. (2). It seems that there is a contradiction between the codes, both conditions can never be fulfilled.

2.4. Model Code 2010

MC2010 (fib 2012) describes robustness as "*the adequate safety in relation with accidental and/or exceptional events"*. Structural (e.g. alternative loading path, capacity design) and non-structural (e.g. reduction of the probability that the action occurs) measures are listed as strategies to reach sufficient robustness.

2.5. WG6T2

In the framework of Eurocode revision, a Technical Regulation (TR) is coming soon. These rules contain the dynamic effect of a sudden column loss, boundary conditions, available rotation capacity, and possible other contributions (O'Connor et al. 2021).

3. EXPERIMENTAL PROGRAM AND TEST SET-UP

3.1. Experimental program

The experimental program consists of four large-scale tests with a span of 3190 mm, width of 450 mm, and a total thickness of 230 mm. The plates differ in the size of bonding surface and the presence of a lattice girder at a distance of 400 mm to the joint (maximum value as prescribed in NBN B 21-606 + A1 (NBN 2019)), see Table 1.

Table 1: Properties of test specimens.

	Surface	Anchor rod
P1	½ steel sheet	/
P2	½ steel sheet	M16
P3	Steel sheet	/
P4	Steel sheet	M20

In two test plates (P2 and P4), the lattice girders 8/5/5 (length of 400 mm and height of 160 mm) are replaced by an outer frame with anchor rods (M16 or M20). To reduce the size of the bonding surface, a thin steel sheet (1 mm) is used to exclude mechanical interlock and adhesion between both concrete phases. Due to the steel sheets, the presence of void formers is simulated and delamination is initiated. The difference in bonding surface and the position of the steel sheets is shown in Figure 1.

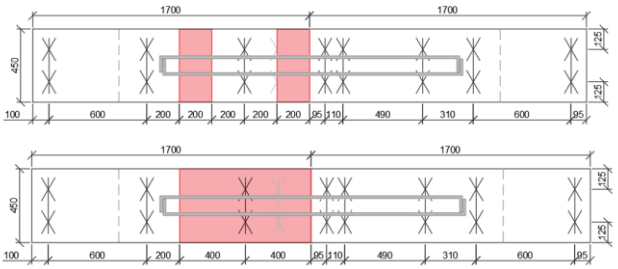

Figure 1: Size of bonding surface (steel sheet = red; upper = ½) (Smits and Van der Wee 2022).

Two overlap bars (Ø16) of 1840 mm provide the transmission of forces between both floor plates. To avoid a pull out failure of the overlap bars, a hook at both ends is applied. The steel properties in Table 2 are delivered by the producer.

Table 2: Steel properties.

	$R_{m,\,mean}/R_{e,\,mean}$ (N/mm²)	σ_m/σ_e (N/mm²)
Lattice girder: upper wire	591/636	2.1/9.5
Lattice girder: lower wire	616/651	5.7/8.4
Overlap bar	537/648	1.0/0.6

3.2. Test set-up

The plates are subjected to a four-point bending test as shown in Figure 2, where the ratio of the distance from the load to the support and the lever

arm is equal to 2.36, to avoid possible beneficial effects of a strut mechanism (CEN 2005).

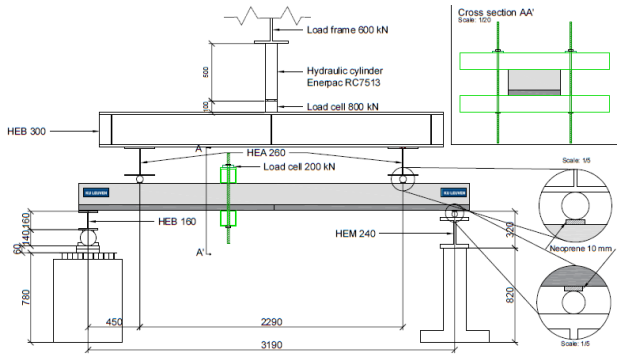

Figure 2: Test set-up (outer frame with anchor rods) (Smits and Van der Wee 2022).

The load is applied by a hydraulic jack force controlled by means of a hydraulic pump and recorded with a load cell. Throughout the tests, the deflection of the plates is measured using linear variable differential transformers (LVDT's), placed at the supports, midspan, and halfway between the supports and midspan.

To detect delamination, vertical strains are measured with DEMEC mechanical strain gages at 30 mm and 95 mm near the joint, with a gage length of 150 mm, and an accuracy of 0.0015 mm. At the levels of the floor plate reinforcement (27 mm from the bottom), joint reinforcement (70 mm from the bottom), and approximately 20 mm from the top, horizontal strains are measured with DEMEC mechanical strain gages (gage length of 200 mm, accuracy of 0.0015 mm). The strain measurements are performed on both sides of the specimens.

Based on the specimen, the measurement method of the force in the first lattice girder near the joint is different. In the case of an outer frame with anchor rods (P2 and P4), the force is measured with a hollow core load cell. When a lattice girder is present (P1 and P3), strain gages are used (*Kyowa*, a gage factor of 2.13 ± 1.0 % and a gage length of 5 mm). In this test campaign, each lattice girder consists of two nodes (eight diagonals). The four diagonals of one node are equipped with two strain gages at each diagonal, as illustrated in Figure 3.

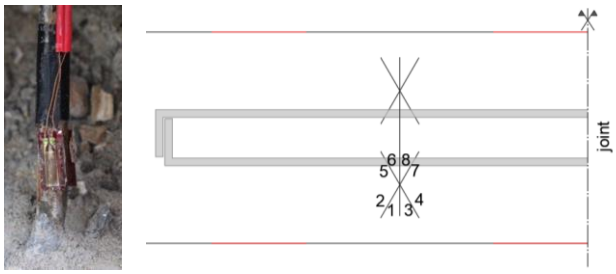

Figure 3: Strain gages (Smits and Van der Wee 2022).

The strain gages are placed as close to the surface of the floor plate as possible. Their position is chosen to take into account the effects of bending of the lattice girder.

4. RESULTS

4.1. Concrete strength

Various compression tests on cubes (150 mm) have been performed, resulting in a mean compression strength of 41.3 N/mm² (f_{cm}) with a standard deviation of 3.3 N/mm² for the floor plates. The mean value of the compression strength for the in-situ poured concrete is 40.2 N/mm² (f_{cm}) with a standard deviation of 5.9 N/mm². By performing splitting tensile tests on cylinders, the mean value of the splitting tensile strength is 3.1 N/mm² ($f_{ct,sp}$) with a standard deviation of 0.3 N/mm².

4.2. Load-deflection curves

Figure 4 shows the load-deflection curves for all the specimens. As can be seen for the P2 test, a large horizontal plateau at equal load is observed. Due to safety issues, the measurement devices have been removed from the other tests before collapse.

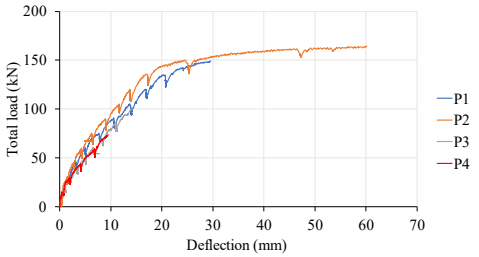

Figure 4: Load-deflection curves for all specimens.

4.3. Strain measurements

The strain measurements on the diagonals of the lattice girder have been converted into forces by making use of Hooke's law, and a constant cross-section. This calculation includes the average of both strain gages per diagonal. The results for P1 and P3 are given in Figure 5, the numbering of the strain gages can be found in Figure 3. Hooke's law is applicable till 10 kN, based on the nominal values of the yield strength (500 N/mm²) and the section of a diagonal (Ø5 mm).

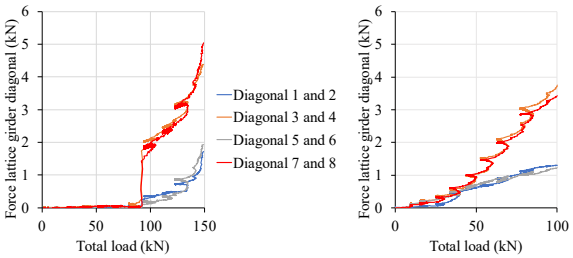

Figure 5: Forces in the diagonals of a lattice girder (P1-half part of the interface covered (left) and P3-fully covered interface area (right)).

The total force acting on a lattice girder is the summation of the forces in each diagonal (eight in total). Because only four diagonals are equipped with strain gages, the result of this force is multiplied by two. Figure 6 shows the results for specimens P1 and P3.

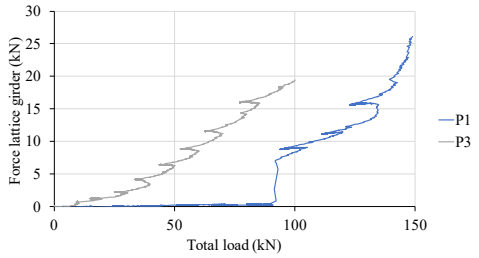

Figure 6: Force in a lattice girder (P1-half part of the interface covered; P3-fully covered interface area).

4.4. Anchor rod measurements

In P2 and P4, the first lattice girder is replaced by an outer frame with anchor rods. The measurements taken from the hollow core load cells are displayed in Figure 7 and Figure 8. The total load in the outer frame is calculated as the sum of both anchor rods.

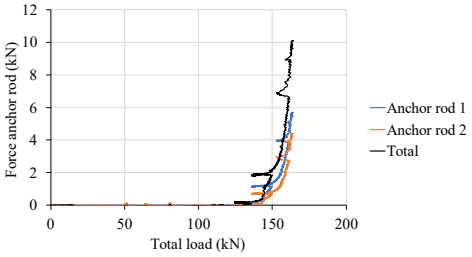

Figure 7: Forces in the anchor rods (P2-half part of the interface covered).

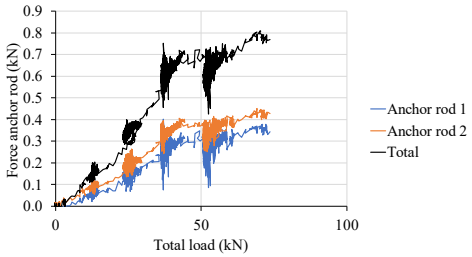

Figure 8: Forces in the anchor rods (P4-fully covered interface area).

4.5. Delamination

Figure 9 shows the occurring delamination in each test. This result is derived from the vertical strain measurements as mentioned before. The strains are measured until one load step before collapse.

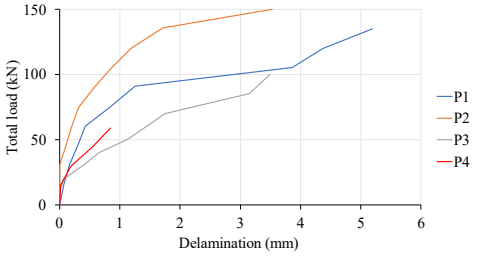

Figure 9: Relation delamination and total force.

Visual observations confirm the ending of delamination at the lattice girder (marked with "T" in Figure 10) located 400 mm near the joint, as illustrated in Figure 10.

Figure 10: 400 mm of delamination.

4.6. Moment-curvature

The moment-curvature relationship, derived out of the horizontal strain measurements, can be used to investigate the ductility of a specimen, as well as the influence on the stiffness of the outer frame measurement method. This relation is shown in Figure 11 for P1 and P2.

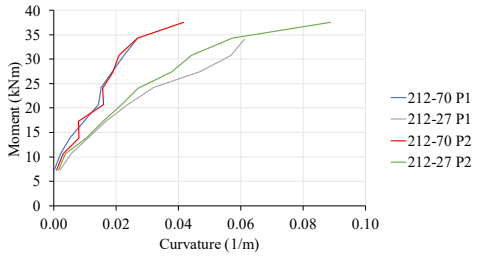

Figure 11: Moment-curvature relationship for P1 and P2.

The curvature can be calculated as the subtraction of the horizontal strains at two levels divided by the distance between them. The curvature of the topping layer is indicated as "212-70" instead of "212-27" in the case of the floor plate.

5. DISCUSSION

5.1. Bending theory

The load-deflection curves in Figure 4 show that the deformations are less than half the height of the specimens (115 mm), so the bending theory remains valid and catenary action is not considered.

5.2. Tensile forces acting on lattice girders

Figure 12 gives a summary of the acting forces.

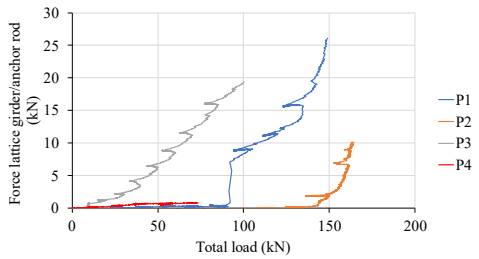

Figure 12: Summary of forces in the lattice girders and anchor rods.

Both lattice girders (each diagonal) and anchor rods are subjected to tensile forces and no compression forces occur. With strain gages, any difference in tension or compression of the diagonals can be measured, which is not possible with anchor rods. NBN EN 1992-1-1 (CEN 2005) mentions the design shear resistance at the interface between concrete cast at different times via formula 6.25, given by Eq. (3). A similar equation can also be found in MC2010 (fib 2012).

$$v_{Rdi} = cf_{ctd} + \mu\sigma_n + \rho f_{yd}(\mu \sin\alpha + \cos\alpha) \leq 0.5\nu f_{cd} \quad (3)$$

The friction factor μ refers to compressive forces, which do not occur in the lattice girders in the detail under consideration. Even though this factor is included in the last part of Eq. (3), which deals with the reinforcement that is crossing the interface (e.g. a lattice girder). This makes the application of this formula questionable in the design of a constructive joint between floor plates.

The forces in the anchor rods in P4 (Figure 8) are in the region of the measurement accuracy of the hollow core load cell. Therefore those measurements can be considered unreliable and will not be discussed. The occurred forces are in contradiction with the existing regulations of (CSTB 2000).

5.3. Measurement methods of forces

Figure 12 shows the difference between the measurements with strain gages and an outer frame with anchor rods. This difference can be attributed to the prevention of deformation caused by the outer frame as illustrated in Figure 11. For an equal value of the bending moment, the curvature of the floor plate is smaller in the case of an outer frame. According to Eq. (4) (M is the bending moment, and R is the radius of curvature), a smaller curvature κ corresponds to a higher value of the bending stiffness EI.

$$\frac{M}{EI} = \frac{1}{R} = \kappa \quad (4)$$

This means that the outer frame provides additional rigidity, which affects the measurement results. In the further continuation, specimens P2 and P4 are therefore omitted due to irrelevance.

5.4. Influence of adhesion

The size of the bonding surface affects the force in a lattice girder as shown in Figure 12. For the same applied load, the acting force on a lattice girder in P3 is higher than in P1. Since less bonding surface is detached in specimen P1 a larger area contributes to the absorption of forces at the interface, reducing the forces in the lattice girder. This means that the lattice girder in P3 is activated immediately after the load has been applied. The lattice girder in specimen P1 (half part of the interface is covered) is activated when adhesive bond is broken. Finally, in both cases, results of the same order of magnitude are obtained. The influence of adhesion is also present in specimens P2 and P4.

5.5. Leverage rule

The diagonals closest to the joint are subjected to higher tensile forces, as depicted in Figure 5. This is expected based on simple leverage rules because when delamination occurs, these diagonals undergo the largest vertical deformations. An estimation is made of the endpoint of delamination by the ratio of the forces in a lattice girder and the distance to this endpoint (a linear elastic behavior is assumed). The calculation shows that this point is close (approximately 35 mm) to the lattice girder, as seen in Figure 10. This validates the statement of (Molkens and Van Gysel 2021) as mentioned before.

5.6. Relation force-delamination

When the concrete phases start to delaminate, there appears to be a quasi-linear relationship between delamination and the force in a lattice girder as seen in Figure 13.

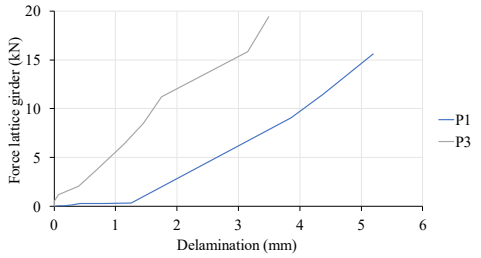

Figure 13: Relation delamination and force lattice girder.

6. CONCLUSIONS

The results of the forces in a lattice girder, which is needed for the design of this element, show that the outer frame method is not capable of reliably capturing all phenomena/failure mechanisms. The design of a lattice girder is not just to avoid horizontal cracks, but to keep these cracks small (adhesion between the concrete phases is lost due to delamination). Strain gage measurements show that higher forces are acting in the diagonals closest to the joint. No compressive forces are recorded during the measurements, which makes the application of formula 6.25 out of NBN EN 1992-1-1 (CEN 2005) not appropriate in the design of the joint. It turns out that the size of the bonding surface affects the moment of activation of a lattice girder.

It can be concluded that a lattice girder is a key element in determining the behavior of the joint and the detailing in case of robustness of concrete composite floors.

Further research is now carried out at KU Leuven, De Nayer Campus, in particular on the behavior under cyclic and impact loading.

7. ACKNOWLEDGEMENTS

The authors would like to express their appreciation to Kerkstoel N.V. (the fabricator of the floor plates) and FEBE (the Belgian Precast Concrete Federation). The experiments have been carried out with the help of my former colleague Jules Van der Wee and lab technician Luc Willems, which are gratefully acknowledged.

8. REFERENCES

Adam, J. M., M. Buitrago, E. Bertolesi, J. Sagaseta, and J. J. Moragues. 2020. “Dynamic performance of a real-scale reinforced concrete building test under a corner-column failure scenario.” *Eng Struct*, 210: 110414. https://doi.org/https://doi.org/10.1016/j.engstruct.2020.110414.

Botte, W., D. Gouverneur, R. Caspeele, and L. Taerwe. 2015. “Influence of Design Parameters on Tensile Membrane Action in Reinforced Concrete Slabs.” *Structural*

engineering international : journal of the International Association for Bridge and Structural Engineering (IABSE), 25 (1): 50–60. ZURICH: Taylor & Francis.

CEN. 2002. *Eurocode 0 Basis of structural design*. Brussels, Belgium: CEN.

CEN. 2005. *Eurocode 2 Design of concrete structures, part 1.1*. Brussels, Belgium: CEN.

CEN. 2006. *Eurocode 1 Actions on structures, part 1.7*. Brussels, Belgium: CEN.

CSTB. 2000. *CPT "Planchers": Cahier des prescriptions techniques communes aux procédés de planchers. Titre II, Dalles pleines confectionnées à partir de prédalles préfabriquées et de béton coulé en oeuvre*. Paris: CSTB.

fib. 2012. *Model Code 2010 - Final draft*.

Gulvanessian, H., and T. Vrouwenvelder. 2006. "Robustness and the Eurocodes." *Structural engineering international : journal of the International Association for Bridge and Structural Engineering (IABSE)*, 16 (2): 167–171. Zürich: Taylor & Francis.

Keyvani, L., and M. Sasani. 2015. "Analytical and Experimental Evaluation of Progressive Collapse Resistance of a Flat-Slab Posttensioned Parking Garage." *J Struct Eng (N Y N Y)*, 141 (11). RESTON: American Society of Civil Engineers.

Linssen, J. 2019. "Oorzaken instorting parkeergarage Eindhoven." *Cementonline*. Accessed January 23, 2023. https://www.cementonline.nl/oorzaken-instorting-parkeergarage-eindhoven.

Michelini, E., P. Bernardi, R. Cerioni, and B. Belletti. 2020. "Experimental and Numerical Assessment of Flexural and Shear Behavior of Precast Prestressed Deep Hollow-Core Slabs." *Int J Concr Struct Mater*, 14 (1): 31. https://doi.org/10.1186/s40069-020-00407-y.

Molkens, T., and A. Van Gysel. 2021. "Structural Behavior of Floor Systems Made by Floor Plates—Mechanical Model Based on Test Results." *Applied Sciences*, 11 (2): 730. https://doi.org/10.3390/app11020730.

Molkens, T., and A. Van Gysel. 2022. "The influence of the interaction surface and reinforcement on the joint capacity of floor slabs made by floor plates." *Concrete Innovation for Sustainability*.

NBN. 2019. *NBN B 21-606+A1:2022 Geprefabriceerde betonproducten - Breedplaten - Nationale toepassingsnorm bij NBN EN 13747+A2:2010 en bij NBN EN 15050+A1:2012*. Brussel: NBN.

O'Connor, A., B. Izzuddin, T. Molkens, B. Belletti, and P. Martinelli. 2021. *Report of project team WG6.T2: Robustness rules in material related Eurocode parts*. Brussels: CEN/TC 250 Mandate M/515.

Sasani, M. 2008. "Response of a reinforced concrete infilled-frame structure to removal of two adjacent columns." *Eng Struct*, 30 (9): 2478–2491. OXFORD: Elsevier Ltd.

Sasani, M., M. Bazan, and S. Sagiroglu. 2007. "Experimental and analytical progressive collapse evaluation of actual reinforced concrete structure." *ACI Struct J*, 104 (6): 731–739. FARMINGTON HILLS: Amer Concrete Inst.

Sasani, M., and S. Sagiroglu. 2010. "Gravity load redistribution and progressive collapse resistance of 20-story reinforced concrete structure following loss of interior column." *ACI Struct J*, 107 (6): 636–644. FARMINGTON HILLS: Amer Concrete Inst.

Smits, J., and J. Van der Wee. 2022. "Weerstand van de constructieve voeg bij breedplaatvloeren: Structurele bijdrage van de tralieliggers." Leuven: KU Leuven. Faculteit Industriële Ingenieurswetenschappen.